Oligomeric State and Mode of Self-Association of *Thermotoga maritima* Ribosomal Stalk Protein L12 in Solution[†]

Pierre D. J. Moens,[‡] Markus C. Wahl,[§] and David M. Jameson*,[‖]

School of Biological, Biomedical, and Molecular Sciences, The University of New England,
Armidale, New South Wales 2351, Australia, Max-Planck-Institut fuer Biophysikalische Chemie, Abteilung Zellulaere Biochemie/
Roentgenkristallographie, D-37077 Goettingen, Germany, and Department of Cell and Molecular Biology,
John A. Burns School of Medicine, University of Hawaii at Manoa, Honolulu, Hawaii 96822

ABSTRACT: The "stalk" of the prokaryotic 50S ribosomal subunit is comprised of four copies of the protein L7/L12. In *Escherichia coli*, L7/L12 is a dimeric protein at micromolar concentrations, which is able to undergo rapid subunit exchange. A recent structural study indicated a tetrameric arrangement of the L12 proteins isolated from *Thermotoga maritima*, in which the proteins engaged in two different dimerization modes. In one mode, the two monomers of L12 form a tight symmetric and parallel dimer held together by a four-helix bundle, which encompasses the hinge region between the N- and C-terminal domains. In the other mode, the two monomers bind through their N-terminal region in an antiparallel configuration, in which one monomer comprises an α-helical hinge and the other monomer adopts an elongated shape with an unfolded hinge region. Presently, it is unclear which dimer contact prevails in solution and on the ribosome. Using cysteine mutants of *T. maritima* labeled with fluorescent probes, we investigated the mode of interactions between L12 subunits. Data from Förster resonance energy transfer experiments support a dimerization of L12 in solution, in which two monomers bind through their N-terminal region in an antiparallel configuration. We also demonstrate that the rate of subunit exchange in *T. maritima* L12 is significantly slower at 25 °C than that in the *E. coli* system. The exchange rate increases with increasing temperature and approaches the one observed for the *E. coli* system at 50 °C. Possible factors responsible for this difference are discussed.

Originally detected 30 years ago in ribosome preparations (*1*), L7/L12 is a small protein of approximately 12 kDa, which together with L10 constitutes the stalk of the 50S ribosome subunit, with L7 being the N-acetylated form of L12 (*2*). L7/L12 is the only ribosomal protein present in multiple copies; specifically, four copies of L7/L12 are present in the 50S ribosomal subunit of *Escherichia coli*. Moreover, L7/L12 is the only ribosomal protein that does not interact with rRNA; its binding to the ribosome is accomplished by its high-affinity interaction with ribosomal protein L10. *In vitro*, L7/L12 and L10 form a pentameric complex with two dimers of L7/L12 (*3*). L7/L12 is necessary for the binding of most of the soluble factors required for protein biosynthesis (*4*) and has been implicated in the control of the translation accuracy (*5*). The protein has two distinct structural domains separated by a flexible hinge. These domains consist of an α-helical N-terminal region and a globular C-terminal region (*6*). A high-resolution crystal

structure of the isolated C-terminal domains from *E. coli* led to a model for a C-terminal domain dimer, which showed direct contacts between these domains based on hydrophobic interactions (*7*). However, steady-state and time-resolved fluorescence studies demonstrated that the two C-terminal domains were, on average, well-separated and highly mobile in the framework of the full-length molecules (*8*, *9*). These conclusions, based on fluorescence studies on L7/L12 in solution, were recently confirmed by NMR studies (*10*, *11*).

Recently, the crystal structure of L12 from the thermophile organism *Thermotoga maritima* (Protein Data Bank IDs 1DD3 and 1DD4) was published (*12*). This structure contained two full-length L12 monomers and two N-terminal fragments (with the C-terminal fragments being unresolved for the latter two monomers). This crystal structure supported the findings, for L7/L12 from *E. coli*, namely, that the interactions between the L12 monomers occur between their N-terminal domains and that their C-terminal domains are well-separated (*6*, *8*, *9*). This study also suggested two possible dimerization modes for the *T. maritima* L12 (*13*, *14*). One of these modes involves a parallel alignment of the two subunits, in which the hinge region adopts an α-helical conformation and the overall protein exhibits a compact shape (Figure 1A). The structure of this dimer was fitted to the electron-density map of the 70S ribosome, but this assignment is tentative, because there is no clear electron

* To whom correspondence should be addressed. E-mail: djameson@hawaii.edu. Telephone: +1 (808) 956-5034. Fax: +1 (808) 956-9952.
[‡] The University of New England.
[§] Max-Planck-Institut.
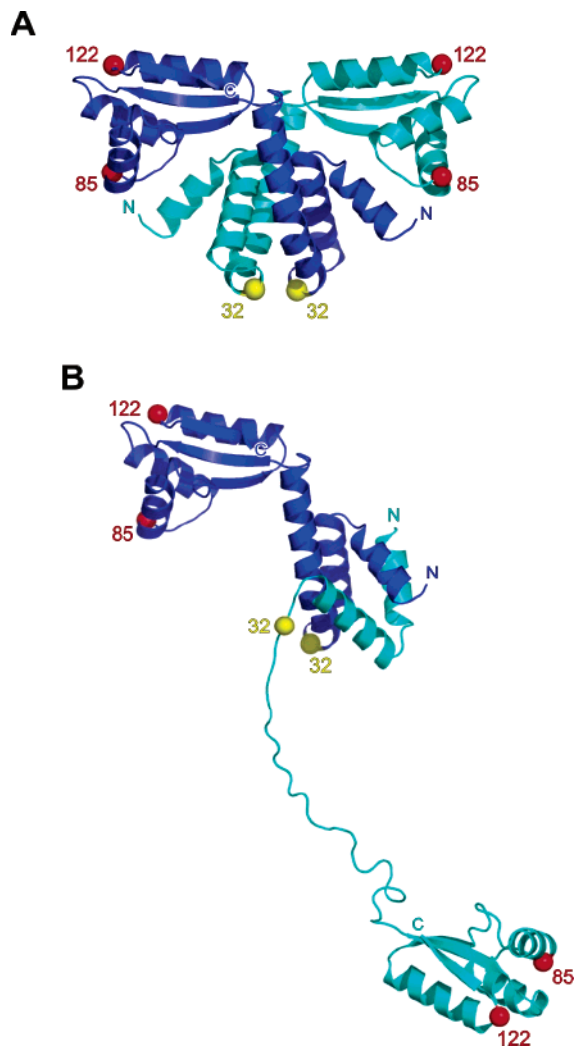[‖] University of Hawaii at Manoa.

FIGURE 1: Dimerization mode of L12. (A) Ribbon representation of the dimer with a parallel alignment of the N-termini. (B) Ribbon representation of the dimer with an antiparallel alignment of the N-termini. Spheres indicate the Cα positions of residues (labeled) used for donor or acceptor probe attachment in the present work. These representations are based on the crystal structure of *T. maritima* L12 (*13*) (Protein Data Bank ID 1DD3) and generated using pyMOL software (DeLano Scientific LLC). The extended model was first proposed by Chandra Sanyal and Liljas (*14*) as the physiological dimerization mode.

density for the L7/L12 proteins (*15*). In the 70S model, only one dimer has been positioned. In 2003, Nomura and colleagues (*16*) also used the compact dimer structure to analyze their point-mutation results of L7/L12.

The second dimerization mode results in an antiparallel arrangement of the four helices of the two N-terminal domains. The hinge region of one subunit curls up into an α-helical structure and aligns with the interacting N-terminal regions to build up a five-helix bundle, while the hinge region of the other subunit adopts an elongated, unfolded configuration. This arrangement (Figure 1B) was favored as the physiological complex by Chandra Sanyal and Liljas (*14*), who proposed that one molecule in the dimer could exhibit a compact structure with a helical hinge region, while the other may exhibit an extended hinge. An extended hinge conformation would allow extensive movement of one of the C-terminal domains. Such an arrangement may allow the C-terminal domains to be recoiled into the stalk structure

part of the time and to extend out of the classic stalk and into the solution at other times. In the present work, we used fluorescence spectroscopy, in particular Förster resonance energy transfer (FRET)[1] to investigate the dimerization mode of *T. maritima* L12 in solution. Our results argue against the existence of L12 tetramers in solution and support the elongated, antiparallel orientation of the subunits for the L12 dimers.

MATERIALS AND METHODS

Cysteine Mutant of L12. Cloning and purification of Ile-to-Cys mutants of L12 were carried out as previously described for other mutants (*12*, *13*). Production of the Cys mutants was based on the original pET22b(+) expression construct, and the cloning and subsequent protein purification steps were as described previously (*12*, *13*).

Protein Labeling. The L12-C32 mutants were labeled with acceptor probe for 2 h at room temperature. Two different "acceptor" probes, dimethylamino-dinitrophenyl maleimide (DABMI) and tetramethyl rhodamine iodoacetamide (TMRIA) were used in a 5 M excess of probe to protein. The labeling was carried out in 50 mM Tris buffer at pH 6.5 for DABMI and pH 8 for TMRIA. The L12-C85 and L12-C122 were labeled with "donor" probes, either iodo-acetamide fluorescein (IAF) or iodoacetylamino-ethylamino naphthalene sulfonic acid (IAEDANS), following the same procedure in 50 mM Tris at pH 8. After labeling, the reaction was stopped by the addition of 1 mM DTT. The free probes were removed by passing the solution through a 5 cm Sephadex G25 column from Pharmacia (previously equilibrated in 50 mM Tris buffer at pH 8) and then further purified by ion-exchange chromatography using a small mono-Q column (Pharmacia). The protein concentration was determined using the BCA assay from Pearce (using BSA as the standard), and the probe concentration was determined by absorption specrophotometry using the following extinction coefficients $(M^{-1} cm^{-1})$: IAEDANS, $\epsilon_{336} = 6100$ (*17*); DABMI, $\epsilon_{460} = 24\,800$ (*18*); and IAF, $\epsilon_{488} = 70\,000$ (*8*). The extinction coefficient for TMRA on the L7 monomer has been determined to be 72 000 $M^{-1} cm^{-1}$ by Hamman et al. (*6*). However, because TMRA-labeled L12-C32 displayed the absorption spectrum typical of a rhodamine ground-state dimer, we used the ratio for TMRA absorption at 518 and 555 nm (518:555 ratio). A ratio of 1.3 represents 100% labeling (*6*). Under these conditions, labeling ratios between 0.9 and 1.1 were found for all cases. Using the same labeling procedures, no labels were detected on the wild-type L12 proteins.

Preparation of the Samples. L12-C32, labeled with the acceptor probe, was mixed with either wild-type L12 or donor-labeled L12 to obtain an acceptor mole fraction (the concentration of acceptor-labeled monomer versus total monomer concentration) of ~0.9. The subunit exchange was followed by polarization measurements, and the FRET measurements were carried out after complete subunit exchange, i.e., more than 2 h after no further changes in the

steady-state polarization could be detected. The final protein concentration was in the range $10-16$ μM.

Fluorescence Spectroscopy: Polarization. Steady-state polarization measurements of fluorescein-labeled L12-C32 were carried out on an ISS PC1 spectrofluorimeter (ISS Inc., Champaign, IL). Excitation of the fluorescein-labeled L12-C32 was at 488 nm, and emission, at wavelengths greater than 515 nm, was observed through a Schott 085 cut-on filter. The excitation bandwidth was set to 4 nm. At the protein concentration used ($10-16$ μM), no significant background due to scattered light or buffer (50 mM Tris at pH 8.0) fluorescence could be detected. The polarization of the sample was recorded every 15 min for 24 h; the sample was only illuminated during the measurement interval. During that time, no photobleaching of the fluorescein moiety could be detected in the control sample of donor-only-labeled L12 (data not shown).

Homo-FRET. Fluorophores that exhibit small Stoke shifts such as fluorescein can undergo homotransfer, which can be detected by the resulting depolarization of the emission ($19-22$). The Förster critical transfer distance (R_0, the distance corresponding to 50% transfer) for fluorescein homotransfer is ~40 Å (9), and hence, significant energy transfer occurs in fluorescein-labeled L12-C32 [because the distances between C32 residues in the N-terminal domains of L12 are within $6-24$ Å, in all cases, i.e., dimer or putative tetramer (13)]. As the proteins within the oligomers exchange with unlabeled L12, the amount of homo-FRET decreases until nearly all of the labeled monomers have formed oligomers with unlabeled monomers (because of the 10-fold excess of unlabeled L12 monomers). Therefore, the exchange of labeled L12 molecules with unlabeled L12 molecules can be followed by polarization measurements as previously described (9).

Hetero-FRET: Determination of the Efficiency of Energy Transfer. Since the solution contains different mixtures of donor- and acceptor-labeled monomers in tetramer and dimers cases, there will be arrangements of the tetramer or dimer consisting of (1) acceptor-labeled monomers only, (2) donor-labeled monomers only, and (3) all possible intermediate combinations (Figure 2). Each arrangement will give rise to a different efficiency of energy transfer, E_k, where k represents a given arrangement and ranges from 1 to 16 for the tetramers and 1 to 4 for the dimers ($23-27$). The efficiency of transfer in any particular arrangement will depend on the number of acceptors present in the assembly as illustrated in Table 1.

In a system corresponding to random monomer assembly, the efficiency of transfer, E, can then be calculated using

$$E = \sum \delta_k E_k \tag{1}$$

where δ_k is the probability for the kth arrangement (Figure 2). This probability is a function of the acceptor molar fraction (~0.9 in this case). Experimentally, the efficiency of transfer between donor and acceptor probes in solution can be determined from the lifetime of the donor probe in the absence (τ_D) and in the presence (τ_{DA}) of the acceptor probe according to the following equation:

$$E = 1 - \frac{\tau_{DA}}{\tau_D} \tag{2}$$

To minimize potential uncertainties with the orientation factor, a parameter embedded in R_0, we used two different donor−acceptor probe pairs. In one case, the donor probe was IAF and the acceptor probe was TMRIA. The R_0 for this probe pair is 55 Å (27). In the second case, the donor probe was AEDANS and the acceptor was DABMI, a nonfluorescent molecule. The R_0 for this latter pair is 43 Å (28). We note that in each case we assume that these R_0 values do not vary among the particular arrangements depicted in Figure 2 (as a consequence of their being in different molecular environments). Since the chemistry of these probes is very different, they may be expected to interact differently with the protein environment. Therefore, if consistent results are obtained between these two probe pairs, we can assume that the orientation factor has a value of $^2/_3$, which corresponds to a random orientation of the dipole moments of the donor and acceptor probes.

Fluorescence Lifetime Determinations. The lifetimes of the fluorophores were determined using an ISS K2 multi-frequency phase and modulation spectrofluorometer (ISS, Inc.) equipped with an Argon-Ion Model 2045 laser (Spectra-Physics, Mountain View, CA). The fluorescein probes were excited at 488 nm, while the 351 nm laser line was used for the AEDANS probes. In the case of fluorescein, the emission was isolated using a combination of a cut-on (Schott 083) and a 513 nm interference filter (Corion), which gave an effective narrow bandpass centered at 528 nm. Under these excitation and emission conditions, the contribution from the acceptor fluorescence was approximately 1%. For the AEDANS emission, wavelengths longer than ~380 nm were observed through a Schott KV399 cut-on filter (note that DABMI, the acceptor for AEDANS, is nonfluorescent). Subtractions of a blank sample containing a mixture of wild-type unlabeled L12 and acceptor-labeled L12 at an acceptor molar ratio of 0.9 and at the same protein concentration as the donor−acceptor or donor-only samples were performed for each measurement. The lifetimes were then analyzed using Globals software available from the Laboratory for Fluorescence Dynamics at the University of Illinois at Urbana−Champaign. While the presence of multiple donor-labeled monomers in a given assembly will not modify the calculations of the efficiency of energy transfer, the presence of multiple donors that do not participate in energy transfer could affect the lifetime analysis. The effect would be larger in the tetramer case compared to the dimer case because only one combination with multiple donors is possible in the latter. To reduce the effect resulting from the presence of multiple donor-labeled monomers in an assembly, we used a high acceptor molar fraction (0.9). The large number of acceptor-labeled monomers means that the probability of having a population of multiple donor-labeled monomers is dramatically reduced and the effect of these donors on the lifetime of the solution becomes negligible. The lifetime analysis is further complicated by the different possible arrangements of labeled monomers in the tetramer and dimer assemblies (Figure 2), which could result in a distribution of lifetimes. Also, because of the mobility of the C-terminal domains, one obtains a distribution of distances and hence lifetimes, in addition to the one obtained from energy transfer. We are thus unable to rigorously relate these lifetime distributions to molecular distributions. Taking these factors into account, as well as the over-interpretation that could result from
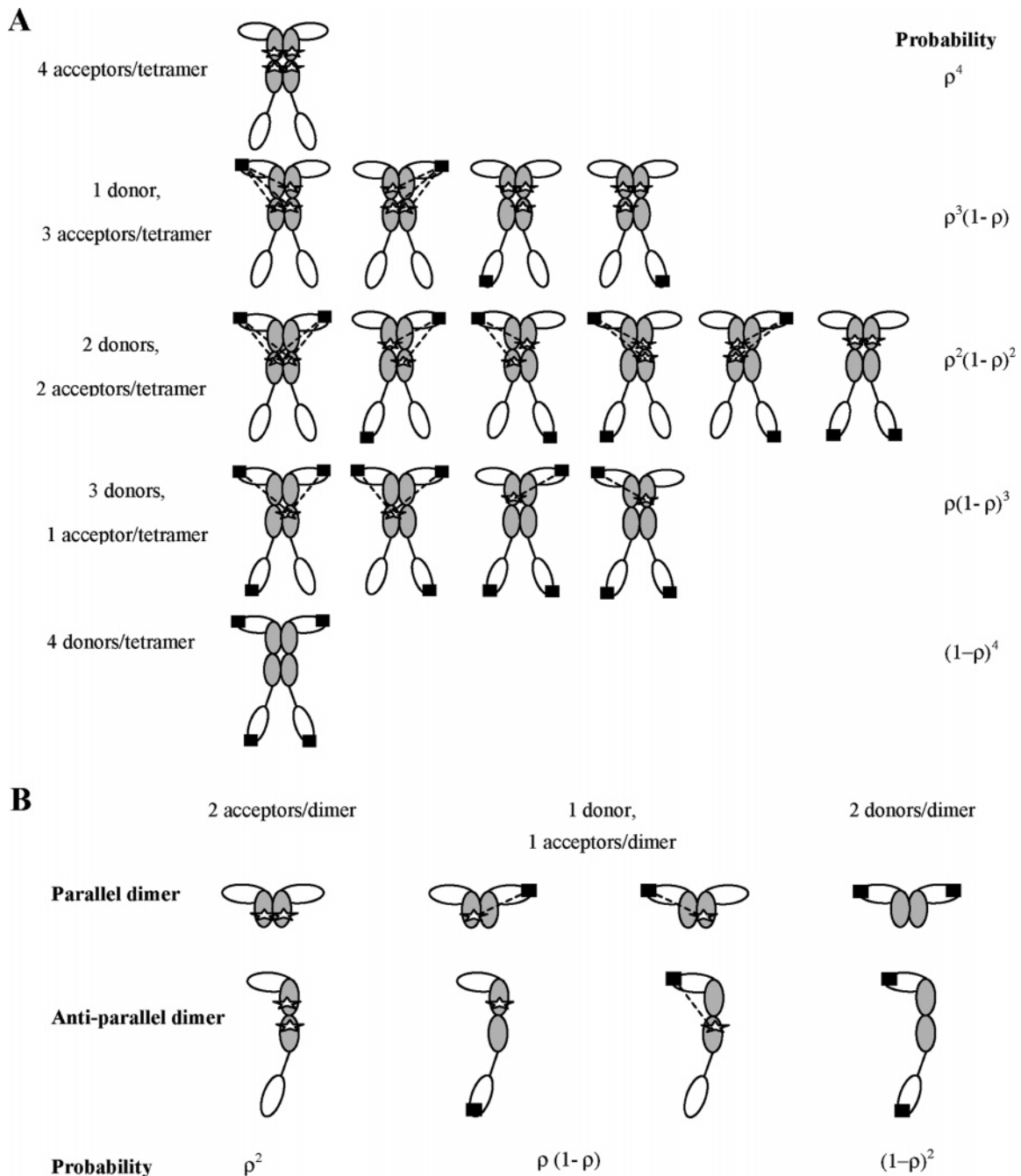
FIGURE 2: Schematic representation of the different arrangements of acceptor- and donor-labeled monomers. The N-terminus of each chain is represented by a shaded oval and the C-terminus, by an open oval. Acceptor probes are represented by stars on the N termini, while donor probes are represented with filled squares on the C termini. The dotted lines indicate the distances where significant energy transfers occur. (A) Tetrameric arrangement. The four chains of the putative tetramer are shown. The probabilities for each of these arrangements are calculated using the formula next to the given arrangement. There is no energy transfer when the tetramer is constituted only of acceptor- or donor-labeled monomers. (B) Dimeric configurations. The probabilities for each of these arrangements are calculated using the formula below the given arrangement. There is no energy transfer when the dimer consists only of acceptor- or donor-labeled monomers.

relating these lifetime distributions to molecular distributions, we decided to fit the data to a single distribution (Lorentzian), and the center values and widths of these distributions are reported.

RESULTS

Oligomerization Mode. Three mutant L12 molecules were employed in the present work: L12-C32, in which residue 32 at the end of the N-terminal dimerization region was exchanged for cysteine and which was used for acceptor probe labeling; and L12-C85 and L12-C122, in which residues 85 and 122 of the C-terminal domain, respectively, were individually exchanged for cysteine to provide a chemical moiety for donor probe labeling. After complete subunit exchange, determined by polarization measurements (see below), the energy transfer between donor- and acceptor-labeled monomers was measured. The lifetime data for the two probe pairs AF-TMRA and AEDANS-DABMI are shown in Table 2. It should be noted that, for donor-only solutions, the lifetimes of both AEDANS and AF probes bound to C85 are longer than the lifetimes of the same probes when attached to C122, which indicates an increase in the

Table 1: Calculation of the Efficiency of Energy Transfer in the Presence of Multiple Acceptor Probes[a]

acceptors only	$E = 0$
donor(s) and three acceptors	$E = \dfrac{R_0^6}{R_0^6 + 1/(R_1^{-6} + R_2^{-6} + R_3^{-6})}$
donor(s) and two acceptors	$E = \dfrac{R_0^6}{R_0^6 + 1/(R_1^{-6} + R_2^{-6})}$
donor(s) and one acceptor	$E = \dfrac{R_0^6}{R_0^6 + 1/R_1^{-6}}$
donors only	$E = 0$

[a] E is the efficiency of energy transfer for the particular arrangement of donors and acceptor probes. R_0^6 is the Förster transfer distance. R_1 is the distance between the donor and the first acceptor probe. R_2 is the distance between the same donor and the second acceptor. R_3 is the distance between the donor and the third acceptor probe.

quantum yield of the fluorophores when bound to C85. In the presence of acceptor-labeled L12, the lifetimes of the donors decreased and the efficiencies of energy transfer ranged from 5 to 8% (Table 2).

Distances between C85-C32 and C122-C32. The published crystal structure of the tetramer of L12 (*13*) reveals distances between the modified residues within the two full-length L12 molecules plus two N-terminal domains. The N-terminal fragments of the structure lack ordered residues for the upper hinge region and the C-terminal domains and thus do not reveal positions of residues 85 and 122 in these molecules. No acceptor probe is located on the monomers labeled with the donor probes and vice versa. Therefore, the reference distances from the crystal structure are between C85 or C122 of a reference molecule (one of the full-length molecules of the crystalline tetramer) and the C32 residues of the other three monomers of the tetrameric assembly (the other full-length molecule and the two N-terminal fragments). These distances were 33, 34, and 35 Å between C85 and C32 residues and 42, 45, and 46 Å between C122 and C32. Taking into account the size of the probes, average distances of 34 and 44 Å for the C32-C85 and C32-C122 cases were used, respectively. On the basis of the representation of the L12 dimer proposed by Chandra Sanyal and Liljas (*14*) (Figure 1B), the distances between C32 and residues C85 and C122 in the C-terminal domains of the two chains that were not resolved in the crystal structure were assumed to be too large for any significant transfer to occur (these distances are in the order of 70−80 Å).

Theoretical Energy-Transfer Calculations for Tetramer and Dimer Models. Since dynamic light scattering, gel-

filtration chromatography, and cross-linking experiments suggested that L12 might exist as a tetramer in solution (*12*), we first calculated the transfer efficiency expected for such a tetramer arrangement. Since there can only be one probe (either the donor or acceptor) per monomer, there are 16 possible arrangements of donor−acceptor probes (Figure 2a).

Using the equations in Table 1 and the average distances determined from the crystal structure, one can calculate the theoretical or expected efficiency of transfer for the 16 arrangements of donor−acceptor probes. Since we assumed that the two unresolved C-terminal domains are too far from the C32s in the N-terminal domains to significantly participate in the energy transfer, we shall ignore the contribution of the donors bound to C85 or C122 in these domains in our FRET calculations. In the determination of the theoretical efficiency of transfer for the distances between C85 and C32, we corrected the R_0 values for the probe pairs due to the increase in quantum yield when the donor probe is linked to C85.

Once the theoretical efficiency of transfer has been calculated for each arrangement, one can calculate the transfer efficiency of the whole solution, which is the sum of the transfer efficiency of each arrangement multiplied by its probability (eq 1). Assuming a random association of the L12 monomers, the probability for each arrangement (Figure 2a) is a function of the acceptor molar fraction (0.9 in these experiments). The values obtained range from 13 to 19% transfer efficiency and are given in Table 2.

Using the same approach, one can calculate the expected transfer efficiencies for the two possible configurations of dimers. In these cases, the number of possible arrangements of donor−acceptor pairs is reduced to 4 as illustrated in Figure 2b. For the parallel dimer, theoretical efficiencies of transfer ranging from 8 to 17% were obtained.

For the antiparallel dimer, similar to the tetramer case, we assumed an absence of energy transfer between the donor probe bound to either C85 or C122 in the unresolved C-terminal domain and the acceptor probes bound to the N-terminal domains. Therefore, the contribution of these donors to the efficiency of transfer can be neglected, and the calculated transfer efficiencies ranged from 4 to 8% (Table 2). These values are in very good agreement with the observed experimental data.

Subunit Exchange. Subunit exchange between fluorescein-labeled L12-C32 and unlabeled proteins was followed by the increase in polarization with time as shown in Figure 3. As stated earlier, this increase resulted from the decrease in homotransfer between the fluorescein moieties after subunit

Table 2: Lifetime and Efficiency of Energy Transfer[a]

donor + acceptor	lifetime (ns)	distribution width (Lorentzian)	FRET efficiency (E)	$E_{theoretical}$ tetramer	$E_{theoretical}$ parallel dimer	$E_{theoretical}$ antiparallel dimer
L12C85-AF + L12 wild type	4.52	0.46				
L12C122-AF + L12 wild type	4.41	0.02				
L12C85-AEDANS + L12 wild type	14.24	4.57				
L12C122-AEDANS + L12 wild type	11.43	0.72				
L12C85-AF + L12C32-TMRA	4.14	0.76	0.08	0.19	0.17	0.08
L12C122-AF + L12C32-TMRA	4.16	0.36	0.06	0.17	0.14	0.07
L12C85-AEDANS + L12C32-DABMI	13.20	4.03	0.07	0.17	0.14	0.07
L12C122-AEDANS + L12C32-DABMI	10.85	0.61	0.05	0.13	0.08	0.04

[a] Lifetime and efficiency of energy transfer (E) for the monomers labeled with the donor probes in the absence and presence of acceptor-labeled monomers and theoretical efficiencies of transfer ($E_{theoretical}$) calculated based on the distances measured on the L12 crystal structure for the different modes of interactions between the monomers.
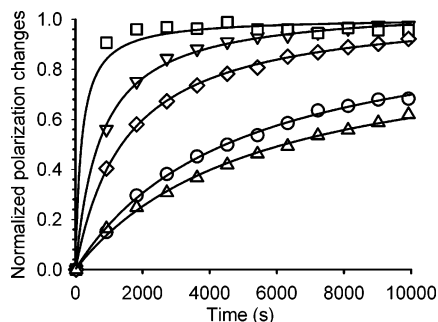
FIGURE 3: Effect of temperature on the L12 exchange rates, monitored by polarization (the polarization data were normalized to facilitate comparisons). The data represent exchange rates for temperature of 20 °C (△), 25 °C (○), 30 °C (◇), 35 °C (▽), and 50 °C (□). The solid lines represent the single-exponential model fitted through the data set from which the rate constants were calculated.
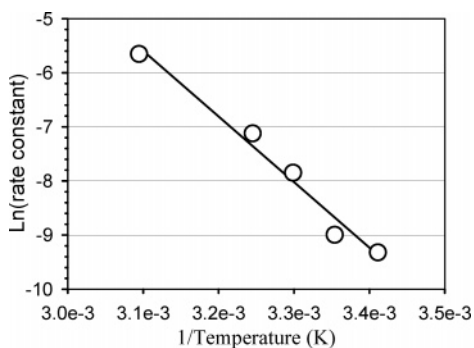

FIGURE 4: Rate constants for the L12 monomer exchanges as a function of the temperature. The data were calculated from the exponential curves in Figure 2. The slope of the regression line fitted through the data gives an estimated energy of activation value of 24 kcal mol^{-1}.

exchange. The polarization corresponding to complete exchange was determined at the plateau region. At 20 °C, the plateau was only reached after 22 h. However, when the temperature of the samples was raised, a proportional increase in the rate of L12 monomer exchange was observed. The rate constants for the exchange were calculated based on fits to single-exponential models and are shown in Figure 4. From the slope of this Arrhenius plot, one can calculate the energy of activation to be about 24 kcal mol^{-1}.

DISCUSSION

In 2000, Wahl and colleagues (*13*) suggested that *T. maritima* L12 formed tetramers in solution compared to *E. coli* L7/L12, which is known to form dimers (*29*). This suggestion was supported by a crystal structure (*13*), but solution measurements were based on hydrodynamic methods (*12*), which are inherently prone to uncertainty because of shape factors. A clear understanding of the solution conformation of *T. maritima* L12 could have implications that bear on the evolutionary differences between L12 molecules from different species and may also be relevant to their interactions with ribosomal protein L10. To study the quaternary structure of *T. maritima* L12 in solution, the protein was labeled with fluorescent probes and subjected to FRET analyses. The amount of energy transfer expected, based on the crystal structure in a tetramer configuration, is much higher (13−19%) than the observed FRET in solution (5−8%). This conclusion is true even when transfers between

the donors in the C-termini of the two unresolved chains and the acceptors at position 32 are neglected. If these residues were participating significantly in energy transfer, the expected FRET efficiency would be even larger. To accommodate the difference in theoretical FRET calculated using the structure of L12 and the FRET efficiency measured in solution, one would have to increase the distances between residue C32 and the residues in the C-terminal domain of L12 (C85 and C122) by 20 Å. These results suggest that L12 from *T. maritima* is not present as a tetramer in solution and that the crystal structure therefore does not represent the solution state of the proteins. The abnormal migration of L12 in analytical gel chromatography, which supported a tetrameric arrangement (*12*), was also observed by Hamman and Jameson (unpublished results) for L7/L12 from *E. coli*, which is known to form dimers in solution (e.g., ref *10*). This unusual migration is presumably due to an elongated average shape of the proteins in solution (*30*) rather than the presence of tetramers. Also, the results obtained by chemical cross-linking could represent transient association of the dimers that were trapped by the cross-linking agent and therefore would not be an accurate representation of the state of the proteins in solution at the concentrations used in the present study. Specifically, the cross-linking experiments were carried out using L12 concentrations in the range of 4−10 mM (*12*). An elongated dimeric arrangement for *E. coli* L7/L12 in solution has recently been visualized by NMR analyses (*10*).

Because the FRET data did not support a tetrameric arrangement of L12, we considered two possible dimerization modes of the proteins. In the first mode, the proteins exhibit a parallel alignment of the two N-terminal domains and the hinge regions adopt an α-helical conformation, which is intimately involved in dimerization. Such dimers display a compact shape. When the expected FRET efficiencies are calculated for this type of dimer, the data obtained (8−17%) are in much better agreement with the observed values in solution (5−8%) than those obtained in the case of the tetramer. However, these values are still too high by a factor of 2. In the second dimerization mode, the proteins adopt an antiparallel alignment of the two N-terminal parts, allowing an extensive movement of one of the C-terminal domains. Assuming no transfer between the unresolved C-terminal portions of one subunit and labeled C32s in the N-terminal part of either subunit, the expected FRET efficiency for this configuration was 4−8%, in very good agreement with the observed efficiency in solution. Our data therefore support this latter dimerization mode of the *T. maritima* L12 proteins. The arrangement that we suggest for the solution state of L12 thus resembles a previous proposition (*14*) and demonstrates that similar structures as in *E. coli* L7/L12 exist in solution (*10*). However, unlike the *E. coli* case, one molecule of the *T. maritima* dimer seems to exhibit an α-helical, recoiled hinge region. Whether this conformation persists on the ribosome remains to be demonstrated.

Having established the dimer nature of the L12 interaction, we investigated the rate of subunit exchange between labeled cysteine mutants of *T. maritima* L12 and wild-type proteins. In *E. coli*, L7/L12 is able to undergo rapid subunit exchange (within a few seconds) (*9*). To our surprise, the rate of exchange of L12 from *T. maritima* was found to be much
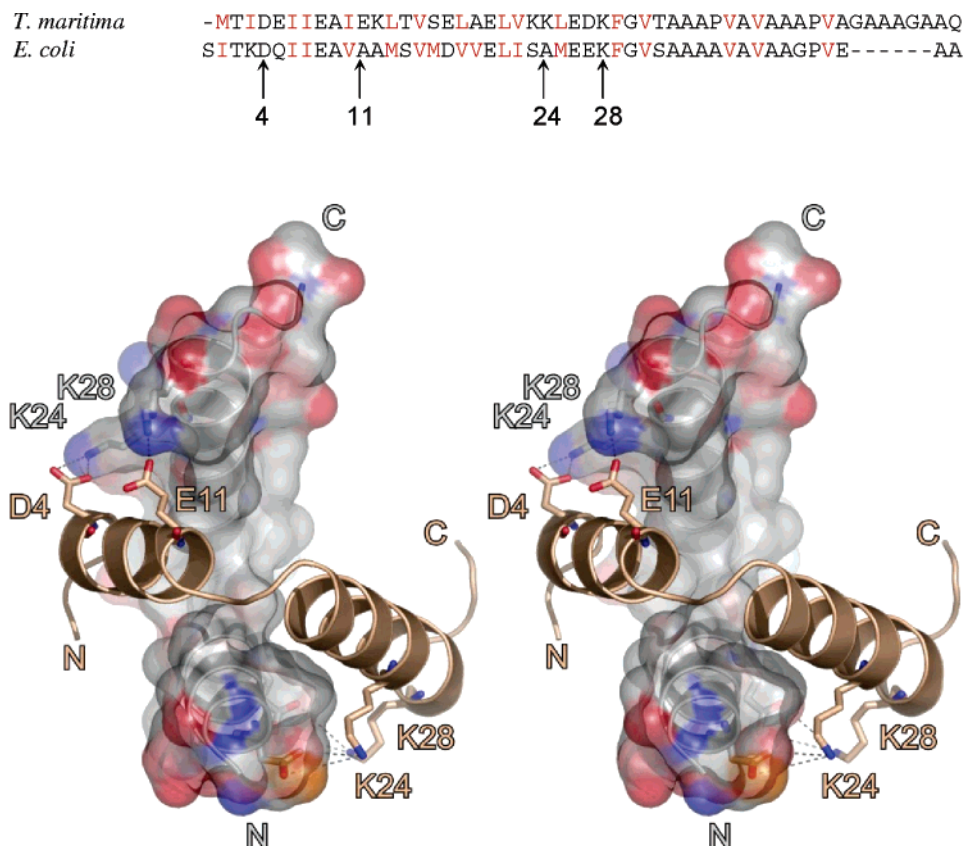
FIGURE 5: Stereoplot of the NTD dimerization region in *T. maritima* L12. Ribbons of the two NTDs are in gray and wheat color. A semitransparent surface for one monomer is shown and color-coded by atom type (carbon, gray; nitrogen, blue; oxygen, red; and sulfur, orange). It is obvious that the central contact area between the monomers is composed of carbon atoms (gray surface in the center), which maintain extensive hydrophobic interactions between the subunits. Four salt bridges are seen in this arrangement (- - -); the residues involved are labeled. The inset on the top shows an alignment of the N-terminal sequence of the L12 proteins from *T. maritima* and *E. coli*. The amino acids in red represent hydrophobic residues. The arrows point at the charged residues in *T. maritima* L12 that are involved in the four salt bridges. The sequence alignment was obtained with ClustalW.

slower (several hours). Although *T. maritima* has an optimal growth temperature of 80 °C, far above the viable temperature for *E. coli*, the *T. maritima* L12 proteins are highly homologous to L7/L12 from *E. coli* (64.7% sequence identity). Interestingly, the lowest sequence identity is found in the N terminus, the site of L12 dimerization (~47% sequence identity in the N-terminal region compared to ~71% sequence identity for the rest of the protein). Possibly, the sequence differences in the N-terminus region stabilize the interaction between *T. maritima* L12 monomers. Such stabilization would therefore allow this L12 protein to function at high temperatures. As illustrated in Figure 5, most of the interactions between the N termini of the monomers are due to hydrophobic residues (Figure 5). All except one of these hydrophobic residues in *T. maritima* correspond to a hydrophobic residue in *E. coli*. However, in *T. maritima*, four residues participate in ionic interactions between the two monomers (D4, E11, K24, and K28). In *E. coli*, E11 and K24 are replaced by alanine residues (inset of Figure 5), resulting in the absence of four ionic bonds. Therefore, we suggest that these ionic bonds are to some extent responsible for the stronger association and the lower exchange rates of L12 from *T. maritima*. Alternatively or in addition to the above mechanism, the stabilization of *T. maritima* L12 dimers relative to their *E. coli* counterparts may be due to unique intersubunit contacts furnished by the α-helical hinge region of one of the molecules (Figure 1B).

It has been demonstrated in the *E. coli* case that the hinge region shows only a very weak tendency to adopt a helical structure (*10*). Thus, in the *E. coli* case, one groove of the five-helix bundle, through which *T. maritima* L12 dimers are maintained, would be left unoccupied, leading to a reduced stability. Consistent with this model, a higher helical content has been detected by circular dichroism measurements in *T. maritima* L12 than those in the *E. coli* homologue (*12*). Experiments are underway to address these questions.

ACKNOWLEDGMENT

REFERENCES

1. Moller, W., and Widdowson, J. (1967) Fractionation studies of the ribosomal proteins from *E. coli*, *J. Mol. Biol. 24*, 367−374.
2. Terhorst, C., Moller, W., Laursen, R., and Wittman-Liebold, B. (1973) The primary structure of an acidic protein from 50S ribosomes of *E. coli* which is involved in GTP hydrolysis dependent on elongation factors G and T, *Eur. J. Biochem. 34*, 138−152.
3. Zecherle, G. N., Oleinikov, A., and Traut, R. R. (1992) The proximity of the C-terminal domain of *Escherichia coli* ribosomal protein L7/L12 to L10 determined by cysteine site-directed mutagenesis and protein−protein cross-linking, *J. Biol. Chem. 267*, 5889−5896.
4. Sommer, A., Etchison, J. R., Gavino, G., Zecherle, N., Casiano, C., and Traut, R. R. (1985) Preparation and characterization of

two monoclonal antibodies against different epitopes in *Escherichia coli* ribosomal protein L7/L12, *J. Biol. Chem. 260*, 6522−6527.

5. Kirsebom, L. A., and Isaksson, L. A. (1985) Involvement of ribosomal protein L7/L12 in control of translational accuracy, *Proc. Natl. Acad. Sci. U.S.A. 82*, 717−721.

6. Hamman, B. D., Oleinikov, A. V., Jokhadze, G. G., Bochkariov, D. E., Traut, R. R., and Jameson, D. M. (1996) Tetramethylrhodamine dimer formation as a spectroscopic probe of the conformation of *Escherichia coli* ribosomal protein L7/L12 dimers, *J. Biol. Chem. 271*, 7568−7573.

7. Leijonmarck, M., and Liljas, A. (1987) Structure of the C-terminal domain of the ribosomal protein L7/L12 from *Escherichia coli* at 1.7 Å, *J. Mol. Biol. 195*, 555−579.

8. Hamman, B. D., Oleinikov, A. V., Jokhadze, G. G., Traut, R. R., and Jameson, D. M. (1996) Rotational and conformational dynamics of *Escherichia coli* ribosomal protein L7/L12, *Biochemistry 35*, 16672−16679.

9. Hamman, B. D., Oleinikov, A. V., Jokhadze, G. G., Traut, R. R., and Jameson, D. M. (1996) Dimer/monomer equilibrium and domain separations of *Escherichia coli* ribosomal protein L7/L12, *Biochemistry 35*, 16680−16686.

10. Bocharov, E. V., Sobol, A. G., Pavlov, K. V., Korzhnev, D. M., Jaravine, V. A., Gudkov, A. T., and Arseniev, A. S. (2004) From structure and dynamics of protein L7/L12 to molecular switching in ribosome, *J. Biol. Chem. 279*, 17697−17706.

11. Mulder, F. A., Bouakaz, L., Lundell, A., Venkataramana, M., Liljas, A., Akke, M., and Chandra Sanyal, S. (2004) Conformation and dynamics of ribosomal stalk protein L12 in solution and on the ribosome, *Biochemistry 43*, 5930−5936.

12. Wahl, M. C., Huber, R., Marinkovic, S., Weyher-Stingl, E., and Ehlert, S. (2000) Structural investigations of the highly flexible recombinant ribosomal protein L12 from *Thermotoga maritima*, *Biol. Chem. 381*, 221−229.

13. Wahl, M. C., Bourenkov, G. P., Bartunik, H. D., and Huber, R. (2000) Flexibility, conformational diversity, and two dimerization modes in complexes of ribosomal protein L12, *EMBO J. 19*, 174−186.

14. Chandra Sanyal, S., and Liljas, A. (2000) The end of the beginning: Structural studies of ribosomal proteins, *Curr. Opin. Struct. Biol. 10*, 633−636.

15. Yusupov, M. M., Yusupova, G. Z., Baucom, A., Lieberman, K., Earnest, T. N., Cate, J. H., and Noller, H. F. (2001) Crystal structure of the ribosome at 5.5 Å resolution, *Science 292*, 883−896.

16. Nomura, T., Mochizuki, R., Dabbs, E. R., Shimizu, Y., Ueda, T., Hachimori, A., and Uchiumi, T. (2003) A point mutation in ribosomal protein L7/L12 reduces its ability to form a compact dimer structure and to assemble into the GTPase center, *Biochemistry 42*, 4691−4698.

17. Hudson, E. N., and Weber, G. (1973) Synthesis and characterization of two fluorescent sulfhydryl reagents, *Biochemistry 12*, 4154−4161.

18. dos Remedios, C. G., Miki, M., and Barden, J. A. (1987) Fluorescence resonance energy transfer measurements of distances in actin and myosin. A critical evaluation, *J. Muscle Res. Cell Motil. 8*, 97−117.

19. Gaviola, E., and Pringsheim, P. (1924) Einfluss der konzentration auf die polarisation der fluoreszenz von farbstofflosenungen, *Z. Physik 24*, 24−36.

20. Weber, G. (1960) Fluorescence polarization spectrum and electronic-energy transfer in proteins, *Biochem. J. 75*, 345−352.

21. Jameson, D. M., Croney, J. C., and Moens, P. D. J. (2003) Fluorescence: Basic concepts, practical aspects, and some anecdotes, *Methods Enzymol. 360*, 1−43.

22. Moens, P. D. J., Helms, M. K., and Jameson, D. M. (2004) Detection of tryptophan to tryptophan energy transfer in proteins, *Protein J. 23*, 89−93.

23. Robinson, J. M., Dong, W. J., and Cheung, H. C. (2003) Can Forster resonance energy transfer measurements uniquely position troponin residues on the actin filament? A case study in multiple-acceptor FRET, *J. Mol. Biol. 329*, 371−380.

24. Moens, P. D., and dos Remedios, C. G. (2001) Analysis of models of F-actin using fluorescence resonance energy transfer spectroscopy, *Results Probl. Cell Differ. 32*, 59−77.

25. dos Remedios, C. G., and Moens, P. D. J. (1999) in *Resonance Energy Transfer* (Andrews, D. L., and Demidov, A. A., Eds.) pp 1−64, John Wiley and Sons Ltd, Chicester.

26. Clegg, R. M. (1996) in *Fluorescence Imaging Spectroscopy and Microscopy* (Wang, X. F., and Herman, B., Eds.) pp 179−252, J. Wileys & Sons, Inc, New York.

27. van der Meer, B. W., Coker, G., and Chen, S.-Y. S. (1991) *Resonance Energy Transfer. Theory and Data*, Wiley-VCH, New York.

28. Moens, P. D., Yee, D. J., and dos Remedios, C. G. (1994) Determination of the radial coordinate of Cys-374 in F-actin using fluorescence resonance energy transfer spectroscopy: Effect of phalloidin on polymer assembly, *Biochemistry 33*, 13102−13108.

29. Gudkov, A. T., Budovskaya, E. V., and Sherstobaeva, N. M. (1995) The first 37 residues are sufficient for dimerization of ribosomal L7/L12 protein, *FEBS Lett. 367*, 280−282.

30. Wong, K. P., and Paradies, H. H. (1974) Shape properties of proteins L7 and L12 from *E. coli* ribosomes, *Biochem. Biophys. Res. Commun. 61*, 178−184.